

# Implications of Martian Rock Distributions on Rover Scaling

Brian Wilcox, Annette Nasif, and Rick Welch  
Jet Propulsion Laboratory  
California Institute of Technology  
4800 Oak Grove Dr.  
Pasadena, CA 91109

## Abstract

This paper discusses some recently published analysis of the rock distribution on Mars and its impact on the scaling of planetary rovers for Mars surface exploration. The images returned by the Viking landers of the mid-1970's showed the Martian surface to be very rocky. (Remote sensing data has indicated that the average rock density over the surface of Mars may be much less than this.) Mathematical models for the rock distribution were proposed in the late 1970's based on power laws. Recently, new analysis has been published which indicates that the number of both small and large rocks was overestimated in the previous model. These models provide the basis for the choice of scale of wheeled rovers; that is, the models provide information which sets the requirements mobility and hazard avoidance systems for the rover at each rover scale. This paper presents the data for the rock distributions at the two Viking landing sites, presents models of rover traversability and navigation as a function of vehicle scale, and discusses the impact on rover hardware, sensing, and control tradeoffs.

## introduction

Analysis of the rock frequency distribution at the Viking landing sites was extensively reported by Moore and others [1,2], and has been recently revisited by Golombek and Rapp [3]. Moore used a power law fit to the data over the range from a few centimeters to about a meter of rock diameter, although he pointed out that this model was valid only over a limited range. Golombek and Rapp have formulated a different law which seems to match the observed data over a wider range. From these results we can extract either the fit to the Viking rock size distributions, or alternatively, use the raw data for the fraction of the surface covered by rocks of average diameter  $D$  or greater at each site to analyze the mobility of alternative planetary rover designs.

Planetary rovers have been considered for several decades, and it is usually paramount in the mind of the engineering team to minimize the overall mission cost, which is usually directly related to the mass of the spacecraft. Microrovers (rovers under about 10Kg in mass) were first proposed in 1987 [4] to address the large cost of planetary exploration missions (which then assumed that rovers approaching 1000 Kg would be sent to Mars). The impact of computation, power, and other system issues on rover scaling has been discussed in the literature [5]. Many alternative vehicle scales have been considered over the years [6], but generally internal system issues have been considered in setting the scale of the vehicles. The effect of scaling on mobility has not been systematically addressed, although it has been generally assumed that large vehicles will always have superior mobility and hazard avoidance properties than smaller vehicles.

One of the key figures of merit in the design of planetary roving vehicles is the "mean free path" of the vehicle in the terrain. This is the expected distance which the vehicle can traverse in a straight line before it encounters a non-traversable hazard. When expressed in units of the vehicle scale (e.g. vehicle turning circle diameter), a large mean free path (e.g.  $\gg 1$ ) means that the terrain is sparsely populated with hazards and that the hazard avoidance algorithm can be very simple and still be effective, since hazards are almost always encountered in isolation. When the mean free path is small (e.g.  $\ll 1$ ), then the terrain is effectively nontraversable for the vehicle, since hazards will be so close together that even short traversable passages will be rare. If the mean free path is moderate (e.g.  $\sim 1$ ) then successful navigation will require elaborate sensing of the terrain and a sophisticated navigation algorithm. Since elaborate sensing and computing performance adds significantly to the cost and complexity of planetary rovers,

reducing the likelihood that such missions will be funded and successful, it is desirable to design rovers which have as large an intrinsic mean free path as possible for the expected terrain within mass and cost constraints. Thus it is useful to consider the Viking landing site data and to compute the mean free path for different vehicle scales and configurations.

### Computing the Mean Free Path

We assume that the vehicle is occupying terrain which is free from hazards, and moves forward a distance  $x$ . We wish to compute  $x$  such that product of the expected number of nontraversable hazards in the swept area of the vehicle out to  $x$  is unity; at this  $x$  the vehicle has reached its mean free path. Hazards are assumed to be distributed randomly, uniformly, and independently, so the distribution of hazards in any area of terrain is a Poisson process with expected value proportional to the area.

Shown in figure 1 is the situation we are considering.

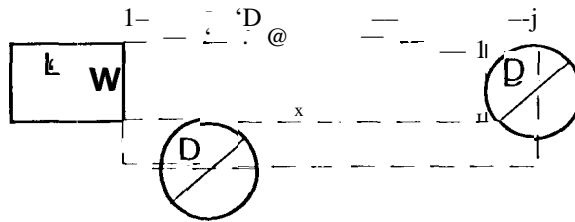


Figure 1. Rover making straight traverse in rock field.

Here a vehicle of length  $L$  and width  $W$  is sitting on the terrain, and preparing to move a distance  $x$  ahead. As can be seen from the figure, when the entire rectangle of length  $x + D/2$  and width  $W + D$  is free from the centers of rocks of diameter  $D$ , the vehicle can move forward by  $x$ . When the expected value of the area of this rectangle multiplied by the areal density of rock centers of diameter  $D$  is unity, then  $x$  is the Mean Free Path. Thus, for all rocks larger than the limiting hazard size  $D_0$ , we have

$$\int_{D_0} (x + D/2)(W + D)\rho(D)dD = 1$$

where  $\rho(D)$  is a probability density which represents the number of rock centers per square meter for rocks with diameters between  $D$  and  $D + dD$ , where  $dD$  is an infinitesimal diameter increment. This can be solved for  $x$  to yield

$$x = \frac{1 - \frac{W}{2} \int_{D_0} D\rho(D)dD - \frac{1}{2} \int_{D_0} D^2\rho(D)dD}{W \int_{D_0} \rho(D)dD + \int_{D_0} D\rho(D)dD}$$

Table 1 gives the numerically generated mean free paths for a Sojourner-like vehicle using the observed rock densities at Viking landing sites 1 and 2 as published in [3] (Sojourner is a rover launched to Mars in Dec 1996 as part of the U.S. Pathfinder mission). Here we have expressed the mean free path not in meters but in terms of the vehicle scale, which we take to be the diameter of the vehicle turning circle  $\sqrt{L^2 + W^2}$ . The vehicles we consider can turn in place, and are therefore limited by their largest diagonal dimension. We have used the estimate that the limiting rock height for Sojourner is equal to its wheel diameter of 13 cm, which is 0.2 times  $L$  and 0.29 times  $W$ ; reference [3] gives the average rock height at VL1 to be about 3/8 of the rock diameter and the average rock height at VL2 to be about 1/2 the rock diameter. These values are used to compute  $L$  and  $W$  for a rescaled Sojourner-like vehicle at each limiting rock diameter  $D_0$  at VL1 and VL2.

$D_0$ limit	VI.1 fract	VI.1	VI.1	VI.1 cum	VI.1 cum	Mean Free	VI.2 fract	VI.2	VI.2	VI.2 cum	VI.2 cum	Mean Free
rock dia.	area	num dens	cum num	weighted	weighted	Path in	area	num dens	cum num	weighted	weighted	Path in
meter (m)	cover>D	$D_i < x < D_{i+1}$	density	by D	by $D^2$	VI.1 terrain	cover>D	$D_i < x < D_{i+1}$	density	by D	by $D^2$	VI.2 terrain
0.9	0.0033	0.005187	0.005187	0.004669	0.004202	45.212	0.0077	(. 012104	0.012104	0.010893	0.009804	13.08738
0.84	0.0033	0	0.005187	0.004669	0.008403	50.21951	0.0143	(ml 191	(.02401 3	0.020897	0.019<08	7.38612
0.76	0.0033	0	0.005187	0.004669	0.008403	5859811	0.0198	0.012124	0.036137	0.030112	0.028011	5.814609
0.72	0.0033	0	0.005187	0.004669	0.008403	63.611s1	0.0247	0.012035	0.048172	0.038777	0.035014	4.783965
0.67	0.0033	0	0.005187	0.004669	0.008403	70.87591	0.0333	(.024393	0.072565	0.05512	0.041253	3.605854
0.63	0.0033	0	0.005187	0.004669	0.008403	77.66327	0.037	0.011869	0.084434	0.062597	0.052203	3.425184
0.56	0.0033	0	0.005187	0.004669	0.008403	92.26943	(.0399	0.011774	0.096208	0.069191	0.056914	3.661971
0.53	0.0033	0	0.0051x7	0.004669	0.008403	99.89157	0.0451	0.02357	0.119778	0.01683	0.060606	3.260893
0.52	0.0084	0.02401S	0.029202	0.0171s6	0.008403	2265339	0.0451	o	0.119778	(.0X1683	0.067227	3.350573
0.5	0.0084	o	0.029202	0.0171s6	0.014897	23.98058	0.0475	(.012223	0.132002	0.087795	0.067227	3.263921
0.48	0.0084	0	0.029202	0.017156	0.014897	25.52112	0.0496	0.011605	0.143607	0.093366	0.070283	3.221698
0.47	0.0084	0	0.029202	0.017156	0.014897	26.349S4	(.05 17	0.0121 04	0.155711	0.0989354	0.072957	3.090509
0.46	0.0108	0.014441	0.043643	0.023799	0.014897	18.84813	0.0537	0.012034	0.167745	0.10459	0.07563	2984283
0.45	0.0108	0	0.043643	0.023799	0.017953	19.4612	0.0557	0.012575	0.18032	0.110249	0.07517 7	2889791
0.43	0.0129	0.014461	0.058104	0.030117	0.0179s3	16.0S233	(.05X9	0.022036	0.202356	0.119724	0.080723	2.795726
0.42	0.0148	0.013714	0.071818	0.035777	0.020626	13.65902	0.0589	0	0.202356	0.119724	0.084798	2.89668
0.41	0.0148	o	0.071818	0.035717	0.023046	14.1s427	0.0605	0.0121 19	0.214475	0.124693	0.084798	2.857179
0.4	0.0167	0.01512	0.086938	0.041825	0.027046	12 32817	(.0605	0	0.214475	0.124693	0.086835	2.968591
0.38	0.0183	0.014108	0.101046	0.0471S6	0.025465	11.60747	0.0646	0.0361S2	0.226626	0.13843	0.086835	2807519
0.37	0.0183	0	0.101046	0.0471 86	0.027502	12.07568	0.0658	0.011161	0.261787	0.14256	0.092055	2.810437
0.36	0.0213	0.029473	0.130519	0.057796	0.027502	9.978323	0.0658	o	0.261787	0.14256	0.093583	2932826
0.35	0.022s	0.01247?	0.142991	0.062 162	0.031322	9.565362	0.067	0.012473	0.274259	0.146925	0.093583	2.945122
0.33	0.0225	o	0.1429s1	0.062 162	0.03285	10.45063	0.068	0.011692	0.285951	0.150783	0.095111	3.115549
0.32	0.0225	0	0.142991	0.06? 162	0.03285	10.94629	0.0718	0.047249	0.3332	0.165903	0.096384	2868618
0.31	0.0225	0	0.142991	0.062162	0.03285	11.47933	0.0736	0.023848	(.357049	(.173296	0.101223	2834797
0.3	0.0235	0.014147	0.157138	0.0664( 16	0.02285	11.12298	0.0771	0.049515	0.406.864	0.188151	0.103514	2.666635
0.29	0.0254	0.028765	0.188904	0.074748	0.034123	10.12605	0.0X02	(.046933	0.453496	0.201761	0.107971	2.553565
0.28	0.0263	0.014616	0.20052	0.078s4	0.036542	9.989218	0.0847	(.073081	0.526578	0.222224	0.111918	2.364919
0.27	0.0288	0.0143664	(.244184	0.09063	0.037688	8899891	0.0867	0.03493 1	0.5615 09	0.271655	(.117647	2361524
0.26	0.0305	0.032019	(.276203	0.098955	(.040871	8.453399	0.0887	0.03767	0.599179	0.241449	0.12(1194	2.366711
0.25	0.0327	0.044818	0.32102 1	0.1101s9	0.043035	7.86396x	0.0899	0.024446	0.623625	0.247561	0.12274	2.429923
0.24	0.0333	0.013263	0.334284	0.113342	0.045837	8063111	0.091	0.024315	0.64794	0.253397	0.124268	2506723
0.23	0.0339	0.014441	0.348725	0.116664	0.04660 1	8.286902	o.0w4	0.072.206	0.720147	0.270004	o.125(W	2.450282
0.22	0.0351	0.031S68	0.380293	0.123609	0.047365	8.231708	0101	0.184146	0.904293	(.130S16	0.1294X8	2.159706
0.21	0.0382	0.089502	0.469795	0.14? 404	0.048892	7.384438	0107	0.17323	1.1(77S23	0.346895	0.13X4(11	1.98698
0.2	0.0408	0.082761	0.552556	0.1589s6	0.052839	6.911548	0.109	0.063662	1.141185	0.359627	0.146041	2.034647
0.19	0.0413	0.017635	0.s70191	0.16? 307	0.05615	7.254711	0.113	0.141079	1.282264	0.386432	(. 148587	1.994141
0.18	0.0439	0.102 [74	0.672364	0.180698	0.056786	6.8572?1	0. 116	0.117893	1.4(0156	0.407653	0.15368	2.009869
0.17	0.0479	0.176227	0.848591	0.210657	0.060697	6139(W	0.119	0.13217	1.532327	0.430122	0.1575	2.034414
0.16	0.0515	0.179049	1.027641	0.239305	0.06519	S.7(17823	0.121	0.099472	1631198	0.446037	0.161319	2.119807
0.15	0.0541	0.14713	1.17477	0.261374	0.069774	5.60679	0.125	0.226354	18S8152	0.47999	0.163866	2.105164
0.14	0.055	0.058465	1.233236	0.2695.S9	0.073084	5.959453	0.13	0.324806	2182958	0.525463	0.1689s9	2.049314
0.13	0.0556	0.045204	1.278439	0.27S436	0.07423	6.455217	0.132	0.1s0679	2333637	0.54s051	0.17532S	2.172399
0.12	0.0577	0.185681	1.46412	0.297717	0.074994	6.530516	0.135	0.265258	2.598896	0.576882	0.177872	2255717
0.11	0.0596	0.19993	1.66405	0.31971	0.077668	6.714093	0.137	(.2 0453	2.809348	0.600032	0.181691	2.423724
0.1	0.0611	0.190986	1.85s036	0.338808	0.080087	7.0!!8616	0.14	0.381972	3.19132	0.638229	0.184238	2.543221
0.09	0.0627	0.251504	2.10654	0.361444	0.081997	7. S23986	0.143	0.47157	3.662891	0.680671	0.188057	2689757
0.08	0.0643	0.31831	2.42485	0.386908	0.084034	8.051338	0.145	0.397887	4.060778	0.712502	0.191877	2.9762?1
0.07	0.0657	0.363783	2788633	0.412373	0.086071	8.830859	0.146	0.259845	4.320623	0.730691	0.194424	3.472667
0.06	0.0678	0.742723	3.531356	0.456937	0.087854	9.371204	0.148	0.707355	5.02797x	0.773132	0.195697	3.938715
0.05	0.0689	0.560225	4091ss1	0.484948	0.090527	10.9766M	0.149	0.509296	5. S37274	0.798597	0.198243	4.815043
0.04	0.0698	0.716197	4.807779	0.5135 96	0.091928	13.51565	0.149	o	s.537274	0.798597	0.199517	6553789
0.03	0.07	0.282942	5.090721	0.522084	0.03074	19.14638	o.149	0	5. S37274	0.798597	0.199517	9.58448

Table 1: Computed Mean Free Paths For Sojourner-like Vehicles in VI.1 and VI.2 Terrain

Note that the mean free path of the vehicles has a minimum of 5.6 vehicle diagonals in VI.1 terrain and at 2.0 vehicle diagonals in VI.2 terrain, for obstacle diameters of 15 cm and 21 cm respectively. The corresponding vehicle dimensions are 28x19 cm for VI.1 and 53x36 cm for VI.2. These represent the "worst" sized vehicles for these terrains, in that they need the most sophisticated hazard sensing and avoidance system to achieve a given level of performance than any other vehicle scale within the range considered. This may be counterintuitive, since one might believe that a larger vehicle will always be able to surmount bigger hazards than a smaller one, and so it is natural to believe that a larger vehicle is always better than a smaller one. For the rock distributions seen at the Viking landing sites, this is not so, since a smaller vehicle can fit between rocks which the larger vehicle would have to surmount. The mean free path is plotted as a function of vehicle length for both VI.1 and VI.2 terrain in Figure 2. Note from Table 1 that the apparent anomaly in the trend of the VI.1 data for large rock diameters is due to the existence of only a single data element in the VI.1 data for large rocks.

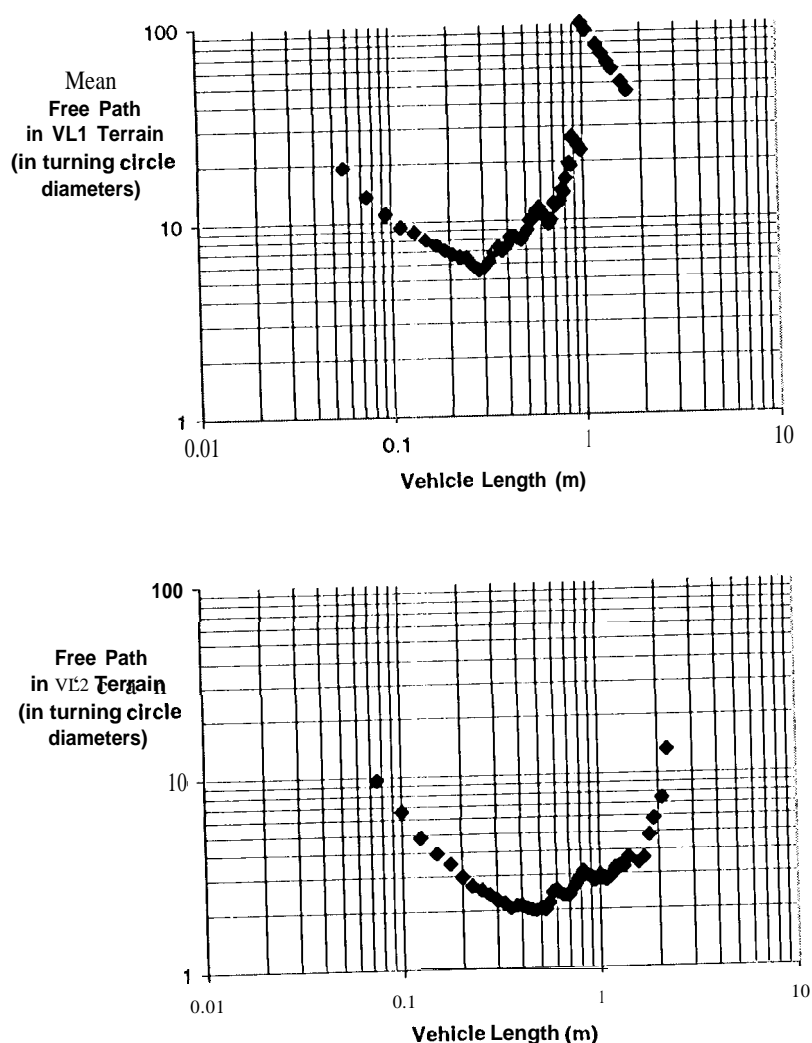


Figure 2. Mean Free Paths of Sojourner-style rovers in VI.1 and VI.2 terrain.

## Effect of Mean Free Path on Navigation Sensing and Control

The mean free path is a critical design parameter in designing the hazard avoidance algorithm. In the case of Sojourner, for example, the hazard avoidance algorithm deals effectively with isolated hazards, but handles pairs of clustered hazards only in a restricted way. (One of the authors [Wilcox] led the activity to develop the hazard avoidance algorithms on Sojourner. Sojourner was designed to have acceptable autonomous navigation performance in V1.1 terrain using an extremely limited 8-bit computer and relatively sparse terrain sensing using 5 laser stripe projectors, but is nominally guided via human-designated waypoints through hazard fields.)

Specifically, due to the limited processing capability of the computer and limited ability of the vehicle to sense hazards at a distance, Sojourner has a small repertoire of behaviors to deal with hazards. The hazard detector has a range just adequate to detect hazards outside the turning circle of the vehicle. If the hazard is on the left, the vehicle turns right. If it is on the right, it turns left. To avoid infinite cycling should a new hazard enter the field of view of the hazard detector, once the vehicle begins turning to avoid a hazard, the vehicle continues to turn in the same direction until a clear path equal to the width of the vehicle turning circle is seen by the hazard sensor. If a gap between two hazards is seen which is wide enough for the vehicle to physically fit between but not big enough to accommodate the vehicle turning circle, then a special behavior called "thread the needle" is instantiated. This behavior centers the vehicle on the perpendicular bisector of the gap, and then moves the vehicle into the gap in a straight line, looking with the hazard sensor until it finds an area large enough to accommodate the vehicle turning circle. If such an area is located before a new hazard which blocks the physical width of the vehicle is detected, then the vehicle forgets its prior state and continues navigating toward the goal. If, on the other hand, some obstacle blocks the vehicle across its physical width, then the vehicle backs straight out in the direction it has come and as far as it has come since the "thread the needle" behavior was instantiated. Since the vehicle has no hazard detection sensors on the rear or side of the vehicle, this is considered a somewhat dangerous maneuver. However, due to the possibility of dense hazards at the Pathfinder landing site, it was deemed essential to have the ability to deal with both isolated hazards as well as pairs of nearby hazards (e.g. those within a vehicle diagonal of each other).

Note that this behavior does not deal effectively with triples of nearby hazards. We can calculate for the V1.1 and V1.2 sites the probability of encountering hazard pairs, triples, or of being blocked completely. Let us examine the case of pairs of hazards shown in Figure 3. Here the vehicle has encountered a first obstacle (with the same conventions used in Figure 1), and without loss of generality (due to mirror symmetry) has maneuvered until its left front corner is adjacent to the hazard. Another hazard will induce the thread-the-needle behavior if it lies far enough from the first hazard that the vehicle will fit between them but close enough to the first hazard that the vehicle turning circle cannot fit between them. So in this case we must compute the probability that another hazard lies in the annulus with inner radius  $W+D$  and with outer radius  $D + \sqrt{L^2 + W^2}$ . Since by assumption the vehicle is passing with the first hazard on the left of the vehicle, we can assume it has turned somewhat to the right and hence that the goal direction is somewhat to the left. Thus the entire quarter-annulus shown in Figure 3 must be considered as a zone in which a hazard of diameter  $D$  will induce the thread-the-needle behavior.

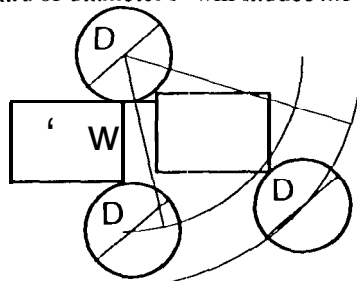


Figure 3. Conditions for Thread-the-Needle behavior to be triggered, showing the two limiting cases.

We can compute the probability that any encounter with a hazard will trigger the thread-the-needle behavior based on the VI.1 and VI.2 rod distributions gives in Table 1. Furthermore, we can compute the likelihood that a thread-the-needle behavior will be successful, or that it will be blocked by a third hazard. Specifically, the probability distribution of the number of rocks in the quarter annulus in Figure 3 is a Poisson distribution with expectation  $\lambda_1$  where

$$\lambda_1 = \int_{D_0}^{\infty} \frac{\pi}{4} ((D + \sqrt{L^2 + W^2})^2 + (W + D)^2) \rho(D) dD$$

which can be computed numerically in the same fashion as in Table 1, and the fraction of hazards encountered which will invoke the thread-the-needle behavior will be  $1 - e^{-\lambda_1}$  (that is, one minus the probability that the Poisson distribution gives no hazards in the quarter annulus). We can further calculate the fraction of thread-the-needle attempts which will be successful (i.e. not blocked by yet a third obstacle). This situation is shown in Figure 4. The vehicle is moving along the perpendicular bisector between the two initial hazards as in Figure 3. A third hazard must not be so close that the vehicle cannot turn in place in the space between the three hazards. With the simple hazard avoidance system on Sojourner this means that there must be no hazard center in a rectangle of width  $W+D$  and length  $(L+D)/2$ . This means that the probability distribution of the number of rocks in the rectangle in Figure 4 is a Poisson distribution with expectation  $\lambda_2$  where

$$\lambda_2 = \int_{D_0}^{\infty} (W + D)(L + D/2) \rho(D) dD.$$

Once again this is computed numerically in the same fashion as in Table 1, and the fraction of thread-the-needle behaviors which are successful is  $e^{-\lambda_2}$ .

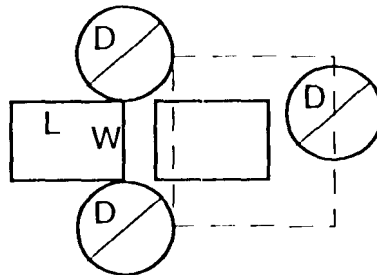


Figure 4. Conditions for Thread-the-Needle behavior to be successful, where the third hazard must be centered outside the dotted rectangle.

The probability that a hazard encountered by the rover will trigger the thread-the-needle behavior is plotted as a function of mean free path in Figure 5. Also plotted is the probability that the thread-the-needle behavior will be successful (i.e. not blocked by a third hazard). Note that the probability of a thread-the-needle behavior becomes high and the probability of success becomes low when the mean free path is much lower (about twice the vehicle turning diameter).

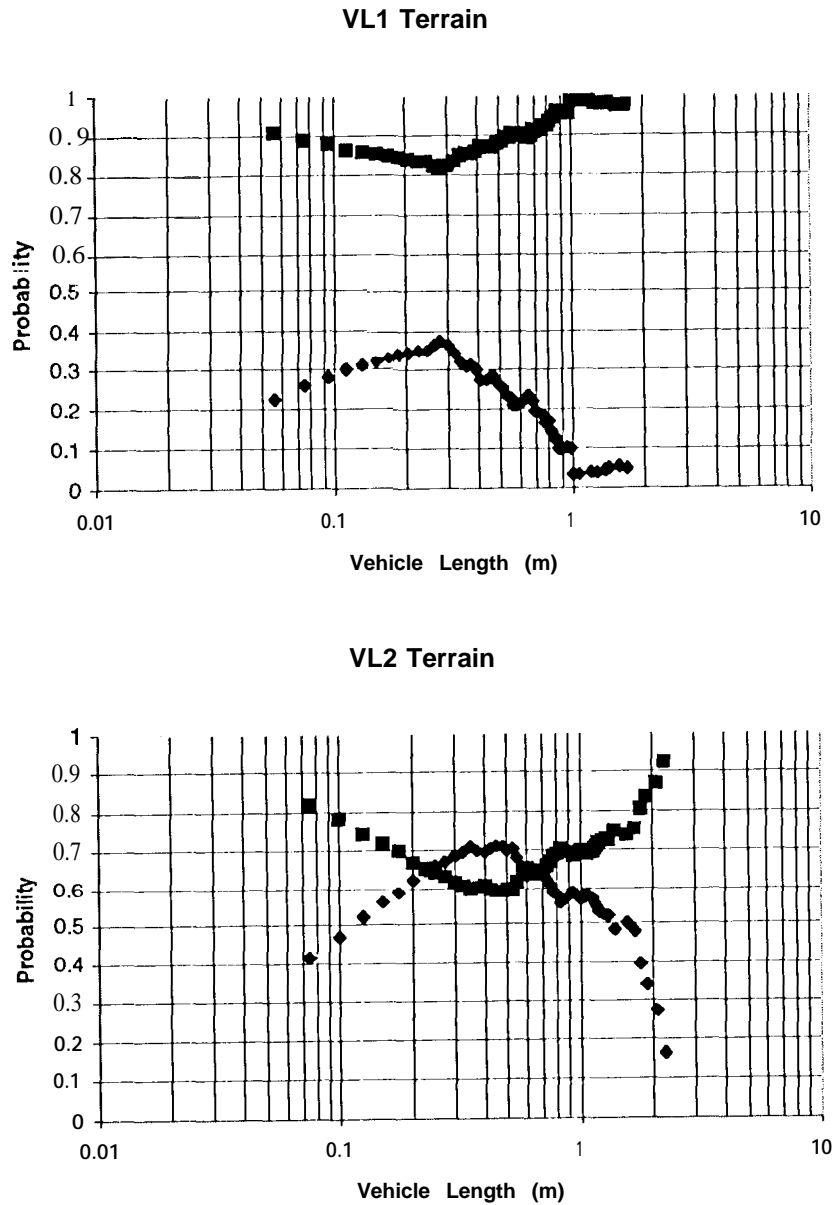


Figure 5. Probability of Thread-the-Needle behaviors (lower curve) and their respective likelihood of success (upper curve) in VL1 and VL2 terrain.

### Discussion and Conclusions

As we have seen, the mean free path for rover vehicles in the rock distributions of the VL1 and VL2 sites has a minimum, and becomes larger for vehicle scales both larger and smaller than about 30-50 cm long. Sojourner was made as small as possible to limit the mass and cost of the mission, and within that scale to be able to surmount the largest hazards possible. Analysis using the Moore power-law fit to the data supported the view that the mobility of vehicles always increased with increasing vehicle size. Note that we would expect that Sojourner (65 cm long) will succeed a thread-the-needle behavior for about 20-25% of the hazards in VL1 terrain and 65% of the hazards in VL2 terrain. We estimate that such behaviors will be successful about 90% of the time in VL1 terrain but only 65% of the time in VL2 terrain. (By

“successful” we mean that the rover is not blocked by a third hazard; if the behavior is unsuccessful, using the Sojourner algorithm, it backs out and searches for another traversable path. Backing out is not a preferred activity on Sojourner since there are no hazard avoidance sensors on the rear of the vehicle.)

Two research tasks at JPL address extending the scale of planetary rovers away from that of Sojourner. One, the Nanorover technology task [7], has built a vehicle with an overall dimension of less than 15 cm (Figure 6). Using the data from Figure 2, we can see that the mean free path for this vehicle (which is expected to have about the same mobility for its size as Sojourner despite having only four wheels due to a novel actively-articulated suspension) is about 8 turning diameters in VI.1 terrain and 4 diameters in VI.2 terrain. This is comparable to the corresponding value for Sojourner in VI.1 terrain, and distinctly better in VI.2 terrain (where Sojourner only has a mean free path of 2-2.5 turning diameters). The effect on the need for advanced hazard sensing and control can be seen in Figure 5, where we see that the Nanorover will need a thread-the-needle behavior for about 32% of the hazards in VI.1 terrain but only 57% of the hazards in VI.2 terrain, and they will be successful 85% of the time in VI.1 terrain and 72% in VI.2 terrain. Thus the Nanorover would be expected to navigate almost as well as Sojourner in VI.1 rock fields and better than Sojourner in VI.2 rock fields. This is one important reason to research the miniaturization of rovers; the mobility performance seems to increase below a critical vehicle scale of about 30 cm. (Of course another important reason to miniaturize rovers is to reduce the overall cost of the missions by reducing the total mass sent to Mars.)



Figure 6. Small rover developed under Nanorover Technology task.

The other research task at JPL, which addresses the issue of rover motility is the Lightweight and Survivable Rover (L.S.R.) task [8]. This task has built a rover with collapsible 20 cm diameter wheels which has an overall length of 1 meter. From Figure 5 we see that such a rover should have much better performance than the Nanorover in VI.1 rock fields, but only about the same performance as the Nanorover in VI.2 rock fields. This surprising result again is due to the ability of the Nanorover to fit between the rocks in VI.2 terrain which the larger rover must surmount.

If the likelihood of thread-the-needle behaviors can be kept low and their likelihood of success kept high, the hazard avoidance system for the rover can be kept rather simple. For example, the benefits which would be derived from having an elaborate planning algorithm or for a long-range hazard mapping capability will be minimal. This is particularly important for nanorovers, since the conventional wisdom would be that the sensing and planning needs of smaller rovers would be greater than those for large rovers even while the difficulty of fitting more advanced sensors and computing into smaller packages grows. Instead, we conclude from Figure 5 that nanorovers can successfully navigate the rock fields seen at VI.1 and VI.2 with simple “isolated hazard” sensing and control if they are made small enough.

Note that this analysis considers only rock-type hazards, and ignores other potential hazards such as dust pits. Regions which appeared to be dust were seen at both Viking landing sites, and these may have been deep enough to engulf small or even large vehicles. No data was returned from Viking about the distribution of the depth of dust seen in these drifts, although it may be that further data on this type of hazard could radically change the conclusions concerning the usability of very small vehicles on the surface of Mars. Both Viking landers did dig with robotic scoops into the nearby regolith; the local dust drifts had cohesion of somewhat more than 1 kPa [9]. This is near the lower limit (being about 0.15 psi) of what is plausible to support larger rovers but it is quite feasible to design nanorovers to this low ground pressure due to the advantageous surface-to-volume ratio at small scales. If dust pits of sufficient depth to engulf small vehicles are very common on Mars, but they infrequently get deep enough to engulf larger vehicles, then it may be that an overall performance metric for vehicles is monotonic with scale. On the other hand it may be that nanorovers can be designed to go over the large drift areas seen in the Viking images (especially at the VI.1 site), which would be a tremendous barrier to the larger vehicles. Thus the conclusion as to the effect of dust on rover mobility and its implications on rover scale must await some physical measurement of the depth distributions of dust drifts, of which Sojourner will make only limited attempts in consideration for its own safety.

### Acknowledgments

The research described in this publication was carried out by the Jet Propulsion Laboratory, California Institute of Technology, under contract with the National Aeronautics and Space Administration.

### References

- [1] Moore, H.J. et al, "Sample Fields of the Viking Landers", *J. Geophys. Res.*, 84, 8365-8377, 1979.
- [2] Moore, H.J. and Jakosky, B. M., "Viking landing sites, remote-sensing observations, and physical properties of Martian surface material", *Icarus*, 81, 164-184, 1989.
- [3] Golombek, M. and Rapp, D. "Size-Frequency Distributions of Rocks on Mars and Earth Analog Sites: implications for Future Landed Missions", *J. Geophysical Res.*, Special Mars Pathfinder Issue, Spring 1997.
- [4] Wilcox, B., "Micro-Lunar-Rover Challenge" *proc. NATO Workshop on Applications of Advanced Sensing to Mobile Robots*, Takeo Kanade, ed., Historil, Portugal, May 1987.
- [5] Wilcox, B. and Gennery, D. "A Mars Rover for the 1990's", *Journal of the British Interplanetary Society*, Vol. 40, No. 10, pp 483-488, Oct 1987.
- [6] Wilcox, B. "Robotic Vehicles for Planetary Exploration", *Journal of Applied Intelligence* 2, pp 181-193, 1992.
- [7] Wilcox, B. et al, "Nanorovers for Planetary Exploration", *proc. AIAA Robotics Technology Forum*, Madison WI, pp 11-1 to 11-6, 1-2 Aug 1996.
- [8] Schenker, P. "New Robotic Technologies for Planetary Surface Science: Developments in Low Mass, Volume Efficient Manipulation and Mobility", *proc. SPIE Conf. on Intelligent Robots and Computer Vision XV*, SPIE proceeds vol 2904, Nov 96.
- [9] Christensen, P.R. and Morley, J. J., "The Martian Surface Layer", *Mars*, Kieffer, Jakosky, Snyder, Matthews, eds, University of Arizona Press, Tucson, pp 687-729, 1992.